Towards a marine biorefinery through the hydrothermal liquefaction of macroalgae native to the United Kingdom

S. Raikova^a, C. D. Le^b, T. A. Beacham^c, R. W. Jenkins^d, M. J. Allen^c, C. J. Chuck^{d*}

Keywords

Macroalgae

Hydrothermal liquefaction

Biorefinery

Bio-crude

Abbreviations

AP – Aqueous phase

ER – energy recovery

HHV - higher heating value

HTG – hydrothermal gasification

HTL - hydrothermal liquefaction

^a Centre for Doctoral Training in Sustainable Chemical Technologies, Department of Chemical Engineering, University of Bath, Claverton Down, Bath BA2 7AY, United Kingdom

^b Department of Oil Refining and Petrochemistry, Hanoi University of Mining and Geology, Hanoi, Vietnam

^c Plymouth Marine Laboratory, Prospect Place, The Hoe, Plymouth PL1 3DH, United Kingdom

^d Department of Chemical Engineering, University of Bath, Claverton Down, Bath BA2 7AY, United Kingdom

Abstract

Hydrothermal liquefaction (HTL) is a promising biomass conversion method that can be incorporated into a biorefinery paradigm for simultaneous production of fuels, aqueous fertilisers and potential remediation of municipal or mariculture effluents. HTL of aquatic crops, such as marine macro- or microalgae, has significant potential for the UK owing to its extensive coastline. As such, macroalgae present a particularly promising feedstock for future UK biofuel production. This study aimed to bridge the gaps between previous accounts of macroalgal HTL by carrying out a more comprehensive screen of a number of species from all three major macroalgae classes, and examining the correlations between biomass biochemical composition and HTL reactivity. HTL was subsequently used to process thirteen South West UK macroalgae species from all three major classes (Chlorophycea, Heterokontophyceae and Rhodophyceae) to produce bio-crude oil, a bio-char, gas and aqueous phase products. Chlorophycea of the genus Ulva generated the highest bio-crude yields (up to 29.9 % for *U. lactuca*). Aqueous phase phosphate concentrations of up to 236 mg L⁻¹ were observed, obtained from the Rhodophyta, S. chordalis. Across the 13 samples, a correlation between increasing biomass lipids and increasing bio-crude yield was observed, as well as an increase in biomass nitrogen generally contributing to biocrude nitrogen content. A broader range of macroalgae species has been examined than in any study previously and, by processing using identical conditions across all feedstocks, has enabled a more cohesive assessment of the effects of biochemical composition.

1 Introduction

The increasing unreliability of crude oil supplies, coupled with the causal link between fossil fuel use, CO₂ emissions and climate change, has led to extensive research into alternative liquid fuel sources compatible with the existing transport infrastructure. The production of first- and second-generation biofuels has been fraught with concerns over effective and ethical utilisation of arable land and fresh water [1], leading to a shift in focus from terrestrial to marine biomass feedstocks. Marine biomass, such as micro- and macroalgae, typically have higher biomass yields [2,3], owing to their higher photosynthetic efficiencies with respect to terrestrial crops (approx. 6–8 %, *c.f.* approx. 1.8–2.2 %) [4]. Although cultivation and harvesting of biomass constitues a roadblock to widespread commercialisation of fuel production technologies [3], micro- and macroalgal fuel production systems also have the potential to be integrated with industrial and municipal waste remediation [5], aquaculture [6–9] or biomining of metals [10] to create an added-value biorefinery.

Investigations into micro- and macroalgae utilisation for biofuel production have spanned anaerobic digestion [11], fermentation [12] and conversion to biodiesel [13,14], with thermochemical processing techniques, such as hydrothermal gasification (HTG), pyrolysis and hydrothermal liquefaction (HTL) attracting attention in more recent years [15]. HTL in particular is ideally suited to wet feedstocks such as micro- and macroalgae, significantly lowering the prohibitive energy requirements associated with feedstock drying [16], and boosting the HHV of the resulting bio-crudes [17] with respect to pyrolysis bio-oils.

HTL utilises water at sub-/near-critical conditions (200–380 °C) as both a solvent and a reactant for a complex cascade of reactions, converting algal biomass into a bio-crude oil, alongside a nutrient-rich aqueous phase, a solid char and gaseous products. HTL of microalgae has been explored in great detail in recent years [18,19] but energy-intensive cultivation and harvesting on an industrial scale remains a major setback to obtaining good energy returns on investment (EROI) [16]. Macroalgal biomass has comparatively lower associated production costs [20] and, as such, has been the subject of a range of recent HTL investigations.

Since the first documented liquefaction of *Macrocystis* sp. [21], a number of different macroalgae species have been examined across all three major classes (Heterokontophyceae, Rhodophyceae and Chlorophyceae – brown, red and green seaweeds) [4,13,22–30]. A comprehensive mechanistic study of microalgae conversion using HTL by Biller and Ross [31] found that biochemical components contributed to bio-crude formation in the order lipids > proteins > carbohydrates proposing a simple additive model for predicting bio-crude yield from biochemical composition. In a similar study examining specifically low-lipid algae, Yang et al. [32] confirmed that proteins made a greater

contribution to bio-crude oil yields than polysaccharides, albeit at the expense of inflated nitrogen content. While this serves as a useful proxy for macroalgae, which tend to contain low lipid and high carbohydrate levels, no macroalgae-specific verification of this relationship has been published to date. Conversely, Elliott et al. have suggested that the oil generated from liquefaction of *Saccharina spp.* is more similar in composition and properties to lignocellulosic HTL bio-crude than the microalgal equivalent [33], despite the almost complete absence of any lignin in the macroalgal feedstock.

A number of investigations [31,34,35] have looked into rationalising HTL reactivity through the use of individual and multiple model compounds, Neveux et al. [27] attempted to use the model proposed by Biller and Ross [31] to predict the bio-crude yields of marine and freshwater Chlorophyceae, but experimentally obtained bio-crude yields did not fit the proposed additive conversion framework. The group speculate that Biller and Ross's model was not an accurate descriptor of the process due to its failure to account for bio-crude generated through secondary reactions between biochemical compounds, in addition to individual additive conversion yields from each biochemical fraction. The occurrence of secondary reactions was confirmed by Jin et al. [36]. In addition to bio-crude oil, hydrothermal liquefaction of marine biomass also generates a range of aqueous products, including water-soluble light organics, ammonia and phosphates. The composition of the aqueous products is dependent on the composition of the feedstock and exact conditions used. The aqueous phase products from HTL of microalgae have been demonstrated to be as effective in promoting growth in microalgal cultures as the industry standard growth media 3N-BBM +V [37]. The recovery of nutrients could prove to be a crucial step in the development of a viable biorefinery, particularly if finite resources, such as phosphorus, are able to be recycled. To date, there has been no assessment of phosphate recovery in the aqueous phase products of macroalgal HTL.

In light of these findings, this investigation aimed to identify optimal conditions for both bio-crude production and nutrient partitioning into the aqueous phase from hydrothermal liquefaction of UK macroalgae species. A comprehensive screening of a range of seaweed species prevalent on the South West coast of the UK was subsequently carried out, and biomass biochemical compositions linked to product yields and properties in order to rationalise reactivity. Based on this, specifications for an ideal biomass feedstock were sought, with the ultimate aim of developing a theoretical model of a South-West UK-based biorefinery for the production of bio-crude oil and fertilisers for terrestrial or microalgal crops.

2 Methods

2.1 Materials and apparatus

Fresh macroalgal biomass samples were collected from Paignton, Devon (specifically, Broadsands Beach 50°24'24.9"N 3°33'16.2"W, Oyster Cove 50°25'04.1"N 3°33'20.9"W and Saltern Cove 50°24'57.9"N 3°33'24.4"W). Prior to analysis, all samples were freeze-dried and milled to <1.4 mm diameter. Samples were stored in sealed vials at -18 °C. Macroalgal species used were *Ascophyllum nodosum* (AN), *Chondrus crispus* (CC), *Fucus ceranoides* (FC), *Fucus vesiculosis* (FV), *Himanthalia elongata* (HE), *Laminaria digitata* (LD), *Laminaria hyperborea* (LH), *Pelvetia canaliculata* (PC), *Rhizoclonium riparium* (RR), *Sargassum muticum* (SM), *Solieria chordalis* (SC), *Ulva intestinalis* (UI) and *Ulva lactuca* (UL). A more detailed description of the collection and preparation of the biomass samples is included in the supplementary information.

Batch reactors were fabricated according to literature precedent using stainless steel Swagelok® tube fittings [31,38,39]. The reactor body consisted of a length of tubing capped at one end, and connected at the other to a pressure gauge, thermocouple, needle valve, and relief valve. The total internal volume of the reactors was *ca.* 50 cm³.

2.2 Procedure

Reaction procedures have been reported previously [39]. In a typical reaction, the reactor was loaded with 4 g biomass and 20 cm³ freshly deionized water, and heated within a vertical tubular furnace set to 400 °C, 550 °C, 700 °C or 850 °C until the specified reaction temperature was reached (300–350 °C, 5–47 min), then removed from the furnace and allowed to cool to room temperature.

After cooling, gaseous products were released *via* the needle valve into an inverted, water-filled measuring cylinder to measure gaseous fraction volume. The gas phase is typically composed of 96–98 % CO₂, observed experimentally for liquefaction of *A. nodosum* at 345 °C, and confirmed by Raikova et al. [39,40]. Hence, gas phase yields were calculated using the ideal gas law, approximating the gas phase as 100 % CO₂, assuming an approximate molecular weight of 44 g mol⁻¹ and a volume of 22.465 dm³ mol⁻¹ gas phase at 25 °C. The yield of gaseous product was determined using the following equation:

yield_{gas} =
$$(V_{gas} \times 1.789 \times 10^{-3}) / (m_{dry biomass}) \times 100 \%$$
 (1)

Following this, the aqueous phase was decanted from the reactor contents and filtered through a Fisher qualitative filter paper pre-dried overnight at 60 °C. The product yield in the water phase was determined by leaving a 2.5 g aliquot to dry in a 60 °C oven overnight, and scaling the residue yield to

the total aqueous phase mass. Aqueous phase residue yield was determined using the following equation:

yield_{AP residue} =
$$m_{\text{residue}}/m_{\text{dry biomass}} \times 100 \%$$
 (2)

To separate the remaining bio-crude oil and char phase, the reactor was washed repeatedly using chloroform until the solvent ran clear, and filtered through the same filter paper used to separate the aqueous phase (after drying for a minimum of 1 h). The filter paper and collected char were washed thoroughly with choloroform to remove all remaining bio-crude. The filtrate was collected, and solvent removed *in vacuo* (40 °C, 72 mbar) until no further solvent evaporation was observed visually, and bio-crude samples were left to stand in septum-sealed vials venting to the atmosphere *via* a needle for a further 12 h to remove residual solvent. Bio-crude yield was determined using the following equation:

yield_{bio-crude} =
$$m_{bio-crude}/m_{dry biomass} \times 100 \%$$
 (3)

The char yield was calculated from the mass of the retentate collected on the filter paper after drying overnight in an oven at 60 °C.

Solid yield was determined using the following equation:

yield_{solid} =
$$m_{\text{solid}}/m_{\text{dry biomass}} \times 100 \%$$
 (4)

Inevitable material losses occurred during work-up, predominantly through evaporation of light organics from the aqueous and bio-crude phases during filtration and solvent removal.

2.3 Biomass and product characterisation

For the macroalgal biomass, lipid quantification was carried out as described previously [38]. Polysaccharide quantification was carried out using the DuBois method [41]as described by Taylor et al. [42], incorporating an upfront two-step hydrolysis protocol adapted from Kostas et al. [43], with polysaccharides quantified on the basis of glucose equivalents.

Elemental analysis was carried out externally at London Metropolitan University on a Carlo Erba Flash 2000 Elemental Analyser to determine CHN content. (Elemental analyses were carried out at least in duplicate for each sample, and average values are reported.) From this, higher heating value (HHV) was calculated using the equation set out by Channiwala & Parikh [44] from elemental composition. Biomass ash was quantified using thermogravimetric analysis (TGA). Approximately 15 mg finely ground biomass was analysed on a Setaram TG-92 Thermogravimetric Analyzer. The sample was heated in air between room temperature and 110 °C at a ramp rate of 10 K min⁻¹, and held for 3–10 min at 110 °C. The mass loss between room temperature and 110 °C was used to determine the sample

moisture content. From 110 °C, the temperature was ramped to 1000 °C at a rate of 10–20 K min⁻¹ and held for 3–120 min, until TG stabilised. The mass remaining at the end of the experiment was taken to be the ash.

For bio-crude and char, elemental analysis and HHV calculations were carried out as described above for the biomass. HHV values calculated using the Channiwal & Parikh equation [44] were found to be in line with values determined experimentally using an IKA C1 bomb calorimeter (within \pm 5%).

A 25 mL sample of the gas phase from liquefaction of *A. nodosum* at 345 °C was analysed using a gas chromatograph (Agilent 7890A) containing an HP-Plot-Q capillary column and fitted with an Agilent 5975C MSD detector. Samples were loaded at 35 °C, held for 7 min at 35 °C, ramped to 150 °C at 20 K min⁻¹, then ramped to 250 °C at 15 K min⁻¹, with a final hold time of 16 min. Helium (1.3 cm³ min⁻¹) was used as the carrier gas.

The concentration of ammonium ions in the aqueous phase was determined using a Randox® urea test kit. The sample was diluted with distilled water to a concentration of 1 % prior to analysis. Urea concentration was calculated relative to a standard solution. From this, ammonium ion concentration was calculated. Aqueous phase total nitrogen was determined by difference, subtracting the total N in the bio-crude and char from the total N in the biomass feedstock (assuming that the N content of the gas phase was negligible). Phosphate concentration in the aqueous phase was determined using a Spectroquant® test kit and photometer system. Prior to analysis, each sample was diluted with deionised water. The total phosphate concentration was determined using a pre-calibrated Spectroquant® photometer.

In order to determine experimental error and test the repeatability of experimental results, three repeat HTL runs of *A. nodosum* were carried out at a range of temperatures between 300–350 °C to determine the standard deviation in mass balances at different reaction temperatures. For ammonia and phosphate quantification, the products of *A. nodosum* liquefaction at 345 °C were analysed in triplicate in all cases to determine standard deviation, and errors assumed to be consistent across different biomass species. All elemental analyses (CHN) were carried out at least in duplicate, and average values used.

3 Results and Discussion

3.1 Optimisation of heating rate and temperature

The effect of heating rate on bio-crude production from HTL of the macroalga *A. nodosum* at 350 °C was examined (Fig. 1a). Variation of heating rates were achieved by changing the furnace temperature: 400 °C, 550 °C, 700 °C and 850 °C set points gave heating rates of 6.7 K min⁻¹, 15.8 K min⁻¹, 34.2 K min⁻¹ and 56.3 K min⁻¹, respectively. Oil yields increased from 18.5 to 20.9 % oil yield on increasing heating rate from 6.7 K min⁻¹ to 15.8 K min⁻¹, slowing progressively on increasing the heating rate to 34.2 K min⁻¹ to give a yield of 21.6 %, increasing modestly to 21.9 % yield on increasing heating rates to 56.3 K min⁻¹.

Although the results confirm the previously identified positive correlation between heating rate and oil production efficiency observed for other biomass types [45,46], the effect was found to become progressively less pronounced at higher heating rates. Furthermore, repeated exposure to furnace temperatures of 850 °C was found to cause damage to reactor fittings. A lower furnace temperature of 700 °C was deemed sufficient to give optimal bio-crude production without compromising reactor integrity. This set point (giving a heating rate of ~30 K min⁻¹) was subsequently used for all HTL experiments.

The effect of HTL reaction temperature on product mass balance was assessed (fig. 1a). Bio-crude oil yields increased with reaction temperature, up to a maximum of 16.3 % (19.5 % on a dry, ash-free basis) at 345 °C. Previously examined macroalgae have given similar results: Anastasakis and Ross [4] obtained the highest yields of bio-crude from *L. saccharina* (19.3 %) at 350 °C, whilst Zhou et al. found that bio-crude yields (23 %) from HTL of *E. prolifera* were highest at 300 °C [24].

The highest overall mass fraction of the product was distributed in the solid phase, predominantly accounted for by the biomass ash (16.2 %). With increasing bio-crude yields, a concomitant decrease in solid products was observed, although a small amount of organic matter from the solid phase also partitioned to the aqueous phase products, which made up the largest product mass fraction on an ash-free basis at temperatures above 310 °C. Material recovery in the gas phase remained relatively stable across the temperature range.

In this investigation, mass balances were determined by measuring the yields of all four product phases, rather than calculating the recovery of one phase by difference. Overall mass closures ranged from 77.2 to 83.9 %. The loss of material is due in part to light organics lost on work-up of the biocrude phase and thermal drying of the aqueous phase to determine residue content. It has also been suggested that some loss could also be attributed to partitioning of oxygen to the aqueous phase in

the form of water [28]. Overall, these mass closures are similar to those observed by Anastasakis and Ross [4] in the hydrothermal processing of *L. digitata*.

Despite the variation in yields, bio-crude elemental compositions (and, consequently, calculated HHV) were unaffected by reaction temperature. All bio-crude HHV values fell between 29.7–32.6 MJ kg⁻¹ (see supporting information). Anastasakis and Ross [4] observed that bio-crude HHV increased slightly on increasing temperatures from 300 °C to 350 °C during the liquefaction of *L. saccharina*, although the degree of experimental error was not specified.

The potential for utilisation of the nutrient-rich aqueous phase from HTL has been explored for microalgae process water [30,37,47]. However, macroalgal HTL process water has yet to be examined. To this end, the concentrations of phosphate and dissolved ammonia in the aqueous phase was analysed with respect to reaction temperature (Fig. 2).

The increase in reaction temperature from 300–350 °C caused phosphate partitioning to the aqueous phase to drop slightly (Fig. 2a), with a simultaneous increase in ammonia concentrations observed (Fig. 2b). Although nutrient levels are still relatively high, they are not as substantial as produced in the aqueous phases from the HTL of most microalgae [39]. Hence, although the aqueous phase products may be of use within a biorefinery paradigm incorporating macroalgal HTL with microalgal cultivation (e.g. for fuels or chemicals), it probably does not represent a higher-value platform than fuel production from bio-crude. Hence, the optimal reaction temperature was selected on the basis of optimising bio-crude oil production, with nutrient recovery presenting a secondary route for product valorisation.

The effect of particle size on the biocrude yield was also examined (Fig. 3). It was found that varying particle size of between $125 \,\mu\text{m} > n \ge 1.4 \,\text{mm}$ did not have a notable effect on bio-crude yield. Given the energy-intensive nature of milling material to a fine particle size on an industrial scale, using the maximum possible particle size is likely to result in significant cost and energy savings. Although additional issues of feedstock processability would need to be addressed for a continuous system at scale, particle sizes of <1.4 mm were deemed appropriate for this investigation. The final conditions taken forward to examine the effect of varying macroalgae feedstock species were a particle size of <1.4 mm, and a reaction temperature of 345 °C, with heating rates of ~30 K min⁻¹.

3.2 Properties of South West UK marine macroalgae

Thirteeen macroalgae species were selected for analysis, belonging to all three major divisions: Rhodophyceae (red macroalgae), Chlorophyceae (green macroalgae) and Heterokontophycea (brown macroalgae).

The proximate, biochemical and ultimate analyses of the seaweed species are presented in table 1. The compositions of many macroalgae generally exhibit pronounced seasonal variation, as well as being strongly affected by growing temperature, geographical location [48], water salinity, and aqueous nutrient content [49], so can differ substantially from samples of the same species grown in alternative climates.

The elemental composition of the macroalgae analysed varied widely, with Chlorophyceae and Rhodophyceae typically containing higher nitrogen and calculated protein than Heterokontophyceae (3–4 % *c.f.* 1–2 % N). Ash was also highly variable, ranging from 10.8 % for *L. hyperborea* to a maximum of 44.5 % for *R. riparium*. *R. riparium*, and *U. intestinalis* had particularly high ash, 20 % on a dry weight basis. Biomass HHV, calculated using the method set out by Channiwala and Parikh [44], ranged between 8.6 MJ kg⁻¹ and 18.2 MJ kg⁻¹, with no obvious dependence on macroalgae division.

Chlorophyceae of the genus *Ulva* and the Heterokontophyceae *A. nodosum* and *P. canaliculata* had the highest lipid (>5 %), which was expected to be beneficial for bio-crude yields. *U. intestinalis, U. lactuca* and the Rhodophyta *C. crispus* had notably high protein contents *ca.* 20 %. This was anticipated to have a positive effect on bio-crude yields, simultaneously increasing ammonia concentrations in the aqueous phase, but possibly having a detrimental effect on bio-crude quality by inflating bio-crude N. High nitrogen levels in crude oil are undesirable: nitrogen-rich fuels generate substantially elevated NO_x emissions on combustion, and nitrogen must therefore be removed through hydrotreatment during the refining process. This can prove somewhat of a setback within a biorefinery context, increasing the energy demand for refining, consuming large quantities of H₂, and posing an increased risk of refinery catalyst poisoning,[27] which must be taken into account for any high-protein feedstocks such as *C. crispus*.

Carbohydrate quantification was carried out using the DuBois method [41]. This method is widely used to quantify carbohydrates in macroalgae, but has the significant drawback of quantifying carbohydrates on the basis of glucose equivalents. Whilst this is highly accurate for simple glucose-based carbohydrates, the method is significantly less sensitive to other monosaccharide units, such as galactose in the common macroalgal carbohydrate carrageenan, or monosaccharides unique to seaweeds, such as mannuronic and guluronic acids present in alginates [43]. Additionally, the method's sensitivity is strongly affected by carbohydrate charge [50]. In this work, analytically

determined soluble carbohydrate is presented alongside estimated total carbohydrate, determined by difference:

$$X_{cabohydrate (tot.)} = 100 \% - (X_{protein} + X_{lipid} + X_{ash})$$
 (5)

Where X_{component} is the mass fraction (%) of each biochemical component.

U. lactuca, S. chordalis and *C. crispus* had the highest analysed carbohydrate, suggesting the presence of high levels of glucose-based polysaccharides. In contrast, the highest total carbohydrate yields as determined by difference were found for the Heterokontophyceae *F. vesiculosis, H. elongata, L. digitata* and *L. hyperborea*, with all four containing >70 % total carbohydrate.

Differences between analysed and calculated carbohydrate were significant for some seaweed species. For example, 71.8 % total carbohydrate was expected for *L. hyperborea*, but only 17.4 % detected. *L. hyperborea* has previously been found to contain significantly higher levels of mannitol (34 %) than the glucose-based polysaccharide laminarin (0.86 %) [51], which may have led to false low readings for total carbohydrate using colourimetric methods based on a glucose standard.. In general, a significant difference (38–55 %) between analysed and calculated carbohydrate was observed for all Heterokontophyceae analysed, suggesting the presence of high levels of non-glucose monosaccharides. Carbohydrate compositions can fluctuate substantially in brown macroalgae, with mannitol alone seen to contribute anywhere between 5 % and 45 % of the dry weight of *L. saccharina* [49] in response to fluctuations in aqueous salinity [52] The analysed and calculated carbohydrate differed to a smaller degree for the Rhodophyceae and Chlorophyceae.

3.3 Liquefaction results

Liquefaction of 13 UK macroalgae species was carried out using the optimised conditions described previously (345 °C; 30 K min⁻¹). Mass balances are summarised in Figure 4, and bio-crude yields are quoted on a dry basis. The highest overall bio-crude yields were obtained for the two macroalgae of the genus *Ulva* (28.8 % and 29.9 % for *U. intestinalis* and *U. lactuca*, respectively), although the third Chlorophyta *R. riparium* performed significantly worse, yielding a modest 15.0 % bio-crude product. *L. digitata* yielded 16.4 % bio-crude – similar to the 17.6 % obtained by Anastasakis and Ross [28], although *L. hyperborea* was found to give 9.8 % bio-crude product in the same study, whereas the macroalgae used in this investigation yielded 12.3 % bio-crude. This can likely be explained by regional and seasonal variations in biomass composition [48,53,54].

Rhodyphyceae gave the highest recoveries of solid products (>45 %), whilst measured gas yields varied substantially (from 5.6 % for *H. elongata* to a maximum of 21.4 % for *L. digitata*). Up to 32.7 % of the feedstock was recovered in the aqueous phase residue (*S. chordalis*), whilst only 5.0 % water-soluble

organic product was generated from *C. crispus*. It has been suggested previously [31] that the presence of high volumes of carbohydrate results in the formation of higher levels of water-soluble polar organics (such as formic, lactic, acetic and acrylic acids formed from the hydrothermal liquefaction of glucose), but aqueous phase residue yields do not appear to reflect this: despite having high analysed and calculated carbohydrate, *U. lactuca*, *U. intestinalis* and *C. crispus* yielded relatively low yields of aqueous phase products (11.4 %, 13.0 % and 5.0 %, respectively), whilst 29.5 % of the feedstock was recovered in the aqueous phase for *H. elongata*, with a comparatively low carbohydrate content of 23.1 %.

Although it was anticipated that higher organic carbon content in the starting biomass would be conducive to obtaining higher bio-crude yields as previously noted [27], there appeared to be no statistically significant correlation between the two parameters. In each case, losses of 4–23 % were encountered. As previously, these are attributed to the loss of volatiles on work-up, and partitioning of oxygen to the aqueous phase in the form of water.

Increasing lipid yields appeared to encourage bio-crude production (Fig. 5a). The correlation between carbohydrate (Fig. 5b) and protein (Fig. 5c) and bio-crude production appeared to be weaker, in line with the observation that lipids are more readily converted to bio-crude than other biochemical components in model studies [31]. To verify these observations, a multiple regression was carried out to quantify the effect of biomass protein, lipid, carbohydrate and ash on bio-crude production. A statistically significant correlation (>95 % confidence) was observed only for lipids. A further regression was carried out for the effect of lipid alone. It was found that variation in biomass lipid accounted for 49 % of the total variation in bio-crude production. The bio-crude yield could be predicted from lipid mass fraction by the following formula:

$$yield_{bio-crude} = 5.71 + 2.6(X_{lipid})$$
 (6)

Where X_{lipid} represents the mass fraction (%) of lipid in the macroalgal biomass.

However, despite the broad correlation, notable exceptions exist in each case: although *U. lactuca* has the highest lipid of the macroalgae analysed (6.9 %), it appears to give a disproportionately high biocrude yield (29.9 %), significantly higher than *A. nodosum*, which gives a yield of 16.0 % with a similar lipid of 6.7 %. As *U. lactuca* has significantly higher protein and measured carbohydrate relative to *A. nodosum*, this may imply that bio-crude yield is positively correlated to overall organic biomolecule content (and hence, negatively correlated to ash), however, no such correlation is observed in practice. The lowest ash was observed for *L. hyperborea* (10.8 %), but a modest bio-crude yield of 12.3 % was obtained. Conversely, a similar yield of 12.9 % bio-crude is obtained from *R. riparium*, despite

an ash content of 44.5 %. In certain cases, ash may play a catalytic role in bio-crude formation, but this is also likely to be due to differences in reactivity between individual lipid, protein and carbohydrate types. Biomass protein was found also to be weakly correlated to bio-crude nitrogen, with the notable exception of *U. lactuca*, which yielded a bio-crude with only 3.8 % N despite containing 24.3 % biomass protein.

An attempt was made to calculate theoretical bio-crude yields using the additive model for bio-crude yield prediction proposed by Biller and Ross [31]:

total theoretical yield bio-crude =
$$(conv._{lipid} \times X_{lipid}) + (conv._{protein} \times X_{protein}) + (conv._{carbohydrate} \times X_{carbohydrate})$$
 (6)

where conv.component represents the theoretical conversion (%) to bio-crude of a given biomass component (lipid, protein and carbohydrate) and X_{lipid}, X_{protein} and X_{carbohydrate} represent the lipid, protein or carbohydrate mass fraction(%) of the feedstock, respectively. The values for theoretical maximum and minimum conversion to bio-crude from individual model lipid, protein and carbohydrate fractions were reported by Neveux et al. [27], who utilised similar feedstocks and processing conditions. Carbohydrate content as determined by difference was used for the calculation of theoretical yields.

Similarly to Neveux et al., this investigation found that predicted maximum yields did not fit well to the model (Fig. 6), with yields under predicted by a wide margin (50–82 %) for the three Chlorophyceae, and over predicted for the remaining feedstocks (by 8–59 %), although the predicted yield was accurate (> 5 % difference) for *F. vesiculosis* and the two Rhodophyceae.

This confirms that the reactivity of a given feedstock under HTL conditions cannot necessarily be inferred from the total levels of lipid, protein and carbohydrate alone. A more complete biochemical breakdown would be necessary to examine mechanistic aspects of bio-crude production, but given the vast number of individual biomolecules within each feedstock, and the variability of biochemical compositions between species, this is likely to be an extremely complex system to analyse. With the large number of potential secondary reactions between primary decomposition products, in practise, when assessing prospective HTL feedstocks for a biorefinery, it will be significantly simpler to determine feedstock suitability experimentally on a case-by-case basis.

All species yielded bio-crudes containing 65–71 % carbon, 7–9 % hydrogen and 3–5 % nitrogen, with the remainder attributed to oxygen, and the HHV of the bio-crudes showed little variation across species, ranging from $28.4-33.0\,\mathrm{MJ\,kg^{-1}}$ (see supporting information), despite the significant variation in biomass biochemical composition, biomass HHV, and bio-crude yields. These crude oils have

approximately 75 % of the energy density of a typical crude oil, and comparable to those obtained for microalgal bio-crude at similar HTL conditions [55]. This effect has been previously observed by Neveux et al. [27] for a range of Chlorophyceae.

The elemental deposition to the bio-oil is presented in Figure 7a. For *U. intestinalis* and *U. lactuca*, carbon recovery in the bio-crude was reasonably high, at 53 % and 57 % respectively. For *C. crispus*, on the other hand the majority of biomass carbon was recovered in the solid phase (see supporting information), with only 13 % in the bio-crude. Although this is unfavourable from a liquid fuel production perspective, energy recovery from bio-char has also been discussed in literature [28]. In this study, while approximately 60 % of the energy from the initial feedstock was retained in the biocrude for *U. lactuca* and *U. intestinalis*, this was reduced substantially to just 14% for *C. crispus* with the majority being found in the solid residue product for this seaweed species (Fig. 7b).

Nitrogen distribution between the products was notably different to that seen for carbon, with the bulk of feedstock N recovered in the aqueous phase, present mainly as NH_4^+ . Although the protein content of *U. intestinalis* and *C. crispus* biomass was almost identical (20.8 % and 20.2 %, respectively), 36 % of the total nitrogen was recovered in the bio-crude for *U. intestinalis*, compared to only 9 % for *C. crispus*. High protein in the feedstock led to partitioning of nitrogen to the bio-crude phase (as well as the aqueous and solid phases), leading to bio-crude nitrogen contents of 3–5 % (see supporting information). The presence of high nitrogen levels in bio-crude is a setback for co-refining operations, increasing the energy demand for refining and posing an increased risk of catalyst poisoning [27], however, the bio-crude nitrogen contents for all feedstocks screened are notably lower than those encountered for bio-crudes obtained from other macroalgae species. Neveux et al. [27] reported bio-crude nitrogen levels from 5.8 % for the marine macroalga *Ulva ohnoi* to 7.1 % for *Cladophora coelothrix*. Both species of *Ulva* analysed in this study gave bio-crudes with lower nitrogen – 3.8 % for *U. intestinalis* and 5.2 % for *U. lactuca* – with the lowest nitrogen content observed for bio-crude from *P. canaliculata* (2.9 %).

Total process energy calculations based on the HHV of the feedstocks and total energy recovery from the bio-crude and char found that in some species a significant amount of energy was being lost to the gaseous and aqueous phase. The energy recovery in the aqueous phase has not been considered at this point, although it is acknowledged that this is theoretically possible if additional processing steps (e.g. hydrothermal gasification) were incorporated [33].

The levels of soluble inorganic nutrients in HTL process water varied significantly with macroalgae species examined (Fig. 8). Ammonia concentrations exceeding 1 g kg⁻¹were observed for *U. intestinalis, L. digitata, L. hyperborea, S. chordalis* and *C. crispus. L. digitata* and *C. crispus* exhibited particularly

high aqueous phase ammonia concentrations, at 2 235 mg kg⁻¹ and 2 415 mg kg⁻¹, respectively. Aqueous phase phosphate concentrations observed were reasonably high, although not as high as those observed for microalgal HTL process water in previous studies [39]. The highest phosphate concentrations (> 100 mg kg⁻¹) were observed for the *F. ceranoides* and *P. canaliculata*. These concentrations are comparable to those found in the standard microalgae growth media, 3N-BBM +V. Process waters with high ammonia and phosphate could be considered for use as a growth supplement for microalgal or macroalgal cultivation, or terrestrial crops, although the effect of the elevated non-ammonia nitrogen (likely to be due to the presence of heterocycles [35]) on plant or algae growth are unclear.

A weak correlation was observed between increasing protein in the biomass feedstock and increasing ammonia concentrations detected in the aqueous phase (Fig. 8b)., though again this was not enough to be able to predict the concentration of NH_4^+ in the aqueous phase.

4 Conclusions

Hydrothermal liquefaction has been demonstrated as an effective technique for the conversion of thirteen UK macroalgae species, nine unexplored in previous literature. Macroalgae of the genus Ulva gave the highest bio-crude yields up to 29.9 %, containing up to 60 % of total biomass energy content. Due in part to low nitrogen in the initial feedstocks, less nitrogen and phosphate were obtained in the aqueous phase compared with microalgal species. As such, with macroalgae, nutrient partitioning into the aqueous phase presents only a minor secondary route for product valorisation, after the reaction conditions have been optimised for bio-crude production. Despite significant variation in biomass elemental and biochemical composition, all bio-crudes produced were similar in elemental composition and HHV. Lipid content was found to account for a substantial proportion of the variation in bio-crude yield. However, feedstock performance could not be predicted from the biochemical breakdown alone. More extensive system modelling, incorporating feedstock-specific components and incorporation of secondary reactions, would be required to identify prospective new feedstock specifications, but in practice, experimentation will be the sole reliable route to assessing feedstock suitability. From the selection of seaweeds assessed, Ulva lactuca, and other members of the family Chlorophyceae, were found to give the best performance for a future biorefinery in the South West region of the UK.

Acknowledgements

The project has been partially supported by the EPSRC through the Centre for Doctoral Training in Sustainable Chemical Technologies (EP/L016354/1), and the RAEng Newton Research Collaboration

Programme (NRCP/1415/176). The authors extend a special thank you to our collaborative partners Rosie and Archie Allen for their invaluable assistance in sourcing the macroalgae species used in this investigation.

References

- [1] K.G. Cassman, A.J. Liska, Food and fuel for all: Realistic or foolish?, Biofuels, Bioprod. Biorefining. 1 (2007) 18–23.
- [2] L. Gouveia, Microalgae and Biofuels Production, in: Microalgae as a Feed. Biofuels, Springer, Heidelberg, 2011: pp. 2–20. doi:10.1007/978-3-642-17997-6.
- [3] J.J. Milledge, P.J. Harvey, Potential process "hurdles" in the use of macroalgae as feedstock for biofuel production in the British Isles, J. Chem. Technol. Biotechnol. 91 (2016) 2221–2234. doi:10.1002/jctb.5003.
- [4] K. Anastasakis, A.B. Ross, Hydrothermal liquefaction of the brown macro-alga Laminaria saccharina: effect of reaction conditions on product distribution and composition., Bioresour. Technol. 102 (2011) 4876–83. doi:10.1016/j.biortech.2011.01.031.
- [5] W.T. Chen, Y. Zhang, J. Zhang, G. Yu, L.C. Schideman, P. Zhang, M. Minarick, Hydrothermal liquefaction of mixed-culture algal biomass from wastewater treatment system into biocrude oil, Bioresour. Technol. 152 (2014) 130–139. doi:10.1016/j.biortech.2013.10.111.
- [6] L. Van Khoi, R. Fotedar, Integration of western king prawn (Penaeus latisulcatus Kishinouye, 1896) and green seaweed (Ulva lactuca Linnaeus, 1753) in a closed recirculating aquaculture system, Aquaculture. 322–323 (2011) 201–209. doi:10.1016/j.aquaculture.2011.09.030.
- [7] E. Marinho-Soriano, S.O. Nunes, M.A.A. Carneiro, D.C. Pereira, Nutrients' removal from aquaculture wastewater using the macroalgae Gracilaria birdiae, Biomass and Bioenergy. 33 (2009) 327–331. doi:10.1016/j.biombioe.2008.07.002.
- [8] S.G. Nelson, E.P. Glenn, J. Conn, D. Moore, T. Walsh, M. Akutagawa, Cultivation of Gracilaria parvispora (Rhodophyta) in shrimp-farm effluent ditches and floating cages in Hawaii: a two-phase polyculture system, Aquaculture. 193 (2001) 239–248. doi:doi:10.1016/S0044-8486(00)00491-9.
- [9] H. Mai, R. Fotedar, J. Fewtrell, Evaluation of Sargassum sp. as a nutrient-sink in an integrated seaweed-prawn (ISP) culture system, Aquaculture. 310 (2010) 91–98. doi:10.1016/j.aquaculture.2010.09.010.
- [10] S. Raikova, C.D. Le, J.L. Wagner, V.P. Ting, C.J. Chuck, Chapter 9 Towards an Aviation Fuel Through the Hydrothermal Liquefaction of Algae, in: C.J. Chuck (Ed.), Biofuels Aviat., Elsevier, London, 2016: pp. 217–239. doi:10.1016/B978-0-12-804568-8.00009-3.

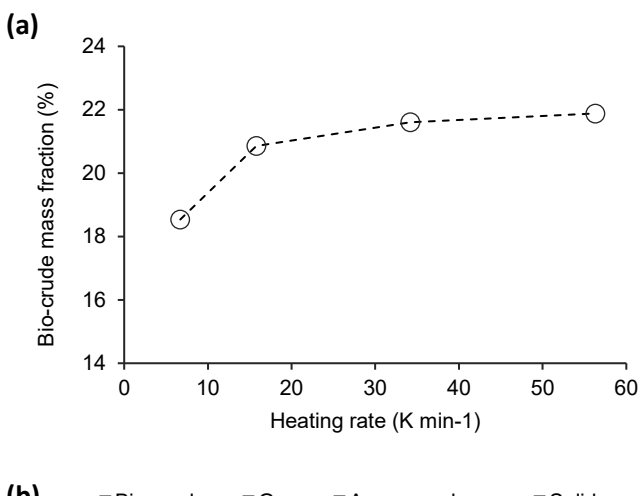
- [11] A. Dave, Y. Huang, S. Rezvani, D. McIlveen-Wright, M. Novaes, N. Hewitt, Techno-economic assessment of biofuel development by anaerobic digestion of European marine cold-water seaweeds, Bioresour. Technol. 135 (2013) 120–127. doi:10.1016/j.biortech.2013.01.005.
- [12] M. Daroch, S. Geng, G. Wang, Recent advances in liquid biofuel production from algal feedstocks, Appl. Energy. 102 (2013) 1371–1381. doi:10.1016/j.apenergy.2012.07.031.
- [13] M. Aresta, A. Dibenedetto, M. Carone, T. Colonna, C. Fragale, Production of biodiesel from macroalgae by supercritical CO2 extraction and thermochemical liquefaction, Environ. Chem. Lett. 3 (2005) 136–139. doi:10.1007/s10311-005-0020-3.
- [14] Y. Chisti, Biodiesel from microalgae., Biotechnol. Adv. 25 (2007) 294–306. doi:10.1016/j.biotechadv.2007.02.001.
- [15] D.C. Elliott, Review of recent reports on process technology for thermochemical conversion of whole algae to liquid fuels, Algal Res. 13 (2016) 255–263. doi:10.1016/j.algal.2015.12.002.
- [16] D.L. Sills, V. Paramita, M.J. Franke, M.C. Johnson, T.M. Akabas, C.H. Greene, J.W. Tester, Quantitative uncertainty analysis of Life Cycle Assessment for algal biofuel production., Environ. Sci. Technol. 47 (2013) 687–94. doi:10.1021/es3029236.
- [17] J. Rowbotham, P. Dyer, H. Greenwell, M. Theodorou, Thermochemical processing of macroalgae: a late bloomer in the development of third-generation biofuels?, Biofuels. 3 (2012) 441–461. doi:10.4155/bfs.12.29.
- [18] D. López Barreiro, W. Prins, F. Ronsse, W. Brilman, Hydrothermal liquefaction (HTL) of microalgae for biofuel production: State of the art review and future prospects, Biomass and Bioenergy. 53 (2013) 113–127. doi:10.1016/j.biombioe.2012.12.029.
- [19] Y. Guo, T. Yeh, W. Song, D. Xu, S. Wang, A review of bio-oil production from hydrothermal liquefaction of algae, Renew. Sustain. Energy Rev. 48 (2015) 776–790. doi:10.1016/j.rser.2015.04.049.
- [20] R. Maceiras, M. Rodrı´guez, A. Cancela, S. Urréjola, A. Sánchez, Macroalgae: Raw material for biodiesel production, Appl. Energy. 88 (2011) 3318–3323.
 doi:10.1016/j.apenergy.2010.11.027.
- [21] D.C. Elliott, L.J. Sealock Jr., S.R. Butner, Product Analysis from Direct Liquefaction of Several High-Moisture Biomass Feedstocks, in: E.J. Soltes, T.A. Milne (Eds.), Pyrolysis Oils From Biomass Prod. Anal. Upgrad. ACS Symp. Ser., American Chemical Society, Washington, D. C., 1988: pp. 179–188. doi:doi:10.1021/bk-1988-0376.ch017.

- [22] J. Wang, G. Wang, M. Zhang, M. Chen, D. Li, F. Min, M. Chen, S. Zhang, Z. Ren, Y. Yan, A comparative study of thermolysis characteristics and kinetics of seaweeds and fir wood, Process Biochem. 41 (2006) 1883–1886. doi:10.1016/j.procbio.2006.03.018.
- [23] A. Ross, J. Jones, M. Kubacki, T. Bridgeman, Classification of macroalgae as fuel and its thermochemical behaviour, Bioresour. Technol. 99 (2008) 6494–6504. doi:10.1016/j.biortech.2007.11.036.
- [24] D. Zhou, L. Zhang, S. Zhang, H. Fu, J. Chen, Hydrothermal Liquefaction of Macroalgae Enteromorpha prolifera to Bio-oil, Energy & Fuels. 24 (2010) 4054–4061. doi:10.1021/ef100151h.
- [25] D. Li, L. Chen, D. Xu, X. Zhang, N. Ye, F. Chen, S. Chen, Preparation and characteristics of biooil from the marine brown alga Sargassum patens C. Agardh, Bioresour. Technol. 104 (2012) 737–742. doi:10.1016/j.biortech.2011.11.011.
- [26] H. Li, Z. Liu, Y. Zhang, B. Li, H. Lu, N. Duan, M. Liu, Z. Zhu, B. Si, Conversion efficiency and oil quality of low-lipid high-protein and high-lipid low-protein microalgae via hydrothermal liquefaction, Bioresour. Technol. 154 (2014) 322–329. doi:10.1016/j.biortech.2013.12.074.
- [27] N. Neveux, A.K.L. Yuen, C. Jazrawi, M. Magnusson, B.S. Haynes, A.F. Masters, A. Montoya, N.A. Paul, T. Maschmeyer, R. de Nys, Biocrude yield and productivity from the hydrothermal liquefaction of marine and freshwater green macroalgae, Bioresour. Technol. 155 (2014) 334–341.
- [28] K. Anastasakis, A.B. Ross, Hydrothermal liquefaction of four brown macro-algae commonly found on the UK coasts: An energetic analysis of the process and comparison with biochemical conversion methods, Fuel. 139 (2015) 546–553. doi:10.1016/j.fuel.2014.09.006.
- [29] D. López Barreiro, M. Beck, U. Hornung, F. Ronsse, A. Kruse, W. Prins, Suitability of hydrothermal liquefaction as a conversion route to produce biofuels from macroalgae, Algal Res. 11 (2015) 234–241. doi:10.1016/j.algal.2015.06.023.
- [30] D. López Barreiro, M. Bauer, U. Hornung, C. Posten, A. Kruse, W. Prins, Cultivation of microalgae with recovered nutrients after hydrothermal liquefaction, Algal Res. 9 (2015) 99– 106. doi:10.1016/j.algal.2015.03.007.
- [31] P. Biller, A.B. Ross, Potential yields and properties of oil from the hydrothermal liquefaction of microalgae with different biochemical con tent., Bioresour. Technol. 102 (2011) 215–25. doi:10.1016/j.biortech.2010.06.028.

- [32] W. Yang, X. Li, Z. Li, C. Tong, L. Feng, Understanding low-lipid algae hydrothermal liquefaction characteristics and pathways through hydrothermal liquefaction of algal major components: Crude polysaccharides, crude proteins and their binary mixtures, Bioresour. Technol. 196 (2015) 99–108. doi:10.1016/j.biortech.2015.07.020.
- [33] D.C. Elliott, T.R. Hart, G.G. Neuenschwander, L.J. Rotness, G. Roesijadi, A.H. Zacher, J.K. Magnuson, Hydrothermal Processing of Macroalgal Feedstocks in Continuous-Flow Reactors, ACS Sustain. Chem. Eng. 2 (2014) 201–215.
- [34] G. Teri, L. Luo, P.E. Savage, Hydrothermal Treatment of Protein, Polysaccharide, and Lipids Alone and in Mixtures, Energy Fuels. 28 (2014) 7501–7509. doi:10.1021/ef501760d.
- [35] P. Biller, R. Riley, A.B. Ross, Catalytic hydrothermal processing of microalgae: decomposition and upgrading of lipids., Bioresour. Technol. 102 (2011) 4841–8. doi:10.1016/j.biortech.2010.12.113.
- [36] B. Jin, P. Duan, Y. Xu, F. Wang, Y. Fan, Co-liquefaction of micro- and macroalgae in subcritical water., Bioresour. Technol. 149 (2013) 103–10. doi:10.1016/j.biortech.2013.09.045.
- [37] P. Biller, A.B. Ross, S.C. Skill, A. Lea-Langton, B. Balasundaram, C. Hall, R. Riley, C. a. Llewellyn, Nutrient recycling of aqueous phase for microalgae cultivation from the hydrothermal liquefaction process, Algal Res. 1 (2012) 70–76. doi:10.1016/j.algal.2012.02.002.
- [38] J. Wagner, R. Bransgrove, T.A. Beacham, M.J. Allen, K. Meixner, B. Drosg, V.P. Ting, C.J. Chuck, Co-production of bio-oil and propylene through the hydrothermal liquefaction of polyhydroxybutyrate producing cyanobacteria, Bioresour. Technol. 207 (2016) 166–174. doi:10.1016/j.biortech.2016.01.114.
- [39] S. Raikova, H. Smith-Baedorf, R. Bransgrove, O. Barlow, F. Santomauro, J.L. Wagner, M.J. Allen, C.G. Bryan, D. Sapsford, C.J. Chuck, Assessing hydrothermal liquefaction for the production of bio-oil and enhanced metal recovery from microalgae cultivated on acid mine drainage, Fuel Process. Technol. 142 (2016) 219–227. doi:10.1016/j.fuproc.2015.10.017.
- [40] Y.-P. Xu, P.-G. Duan, F. Wang, Hydrothermal processing of macroalgae for producing crude bio-oil, Fuel Process. Technol. 130 (2015) 268–274. doi:10.1016/j.fuproc.2014.10.028.
- [41] M. DuBois, K. Gilles, J. Hamilton, P. Rebers, F. Smith, Colorimetric method for determination of sugars and related substances, Anal. Chem. 28 (1956) 350–356.
- [42] K.A.C.C. Taylor, A modification of the phenol/sulfuric acid assay for total carbohydrates giving more comparable absorbances, Appl. Biochem. Biotechnol. 53 (1995) 207–214.

- doi:10.1007/BF02783496.
- [43] E.T. Kostas, S.J. Wilkinson, D.A. White, D.J. Cook, Optimization of a total acid hydrolysis based protocol for the quantification of carbohydrate in macroalgae, J. Algal Biomass Util. 7 (2016) 21–36.
- [44] S.A.A. Channiwala, P.P.P. Parikh, A unified correlation for estimating HHV of solid, liquid and gaseous fuels, Fuel. 81 (2002) 1051–1063. doi:10.1016/S0016-2361(01)00131-4.
- [45] J.L. Faeth, P.J. Valdez, P.E. Savage, Fast Hydrothermal Liquefaction of Nannochloropsis sp. To Produce Biocrude, Energy & Fuels. 27 (2013). doi:10.1021/ef301925d.
- [46] B. Zhang, M. von Keitz, K. Valentas, Thermal Effects on Hydrothermal Biomass Liquefaction, Appl. Biochem. Biotechnol. 147 (2008) 143–150.
- [47] U. Jena, N. Vaidyanathan, S. Chinnasamy, K.C. Das, Evaluation of microalgae cultivation using recovered aqueous co-product from thermochemical liquefaction of algal biomass, Bioresour. Technol. 102 (2011) 3380–3387. doi:10.1016/j.biortech.2010.09.111.
- [48] H.M. Khairy, S.M. El-Shafay, Seasonal variations in the biochemical composition of some common seaweed species from the coast of Abu Qir Bay, Alexandria, Egypt, Oceanologia. 55 (2013) 435–452. doi:10.5697/oc.55-2.435.
- [49] P.D. Kerrison, M.S. Stanley, M.D. Edwards, K.D. Black, A.D. Hughes, The cultivation of European kelp for bioenergy: Site and species selection, (2015). doi:10.1016/j.biombioe.2015.04.035.
- [50] A.A. Albalasmeh, A.A. Berhe, T.A. Ghezzehei, A new method for rapid determination of carbohydrate and total carbon concentrations using UV spectrophotometry, Carbohydr. Polym. 97 (2013) 253–261. doi:10.1016/j.carbpol.2013.04.072.
- [51] A. Graiff, W. Ruth, U. Kragl, U. Karsten, Chemical characterization and quantification of the brown algal storage compound laminarin — A new methodological approach, J. Appl. Phycol. 28 (2016) 533–543. doi:10.1007/s10811-015-0563-z.
- [52] R.H. Reed, I.R. Davison, J.A. Chudek, R. Foster, The osmotic role of mannitol in the Phaeophyta: an appraisal, Phycologia. 24 (1985) 35–47.
- [53] E. Marinho-Soriano, P.C. Fonseca, M. a a Carneiro, W.S.C. Moreira, Seasonal variation in the chemical composition of two tropical seaweeds, Bioresour. Technol. 97 (2006) 2402–2406. doi:10.1016/j.biortech.2005.10.014.

- [54] J.M.M. Adams, A.B. Ross, K. Anastasakis, E.M. Hodgson, J.A. Gallagher, J.M. Jones, I.S. Donnison, Seasonal variation in the chemical composition of the bioenergy feedstock Laminaria digitata for thermochemical conversion, Bioresour. Technol. 102 (2011) 226–234. doi:10.1016/j.biortech.2010.06.152.
- [55] D. López Barreiro, C. Zamalloa, N. Boon, W. Vyverman, F. Ronsse, W. Brilman, W. Prins, Influence of strain-specific parameters on hydrothermal liquefaction of microalgae., Bioresour. Technol. 146 (2013) 463–71. doi:10.1016/j.biortech.2013.07.123.



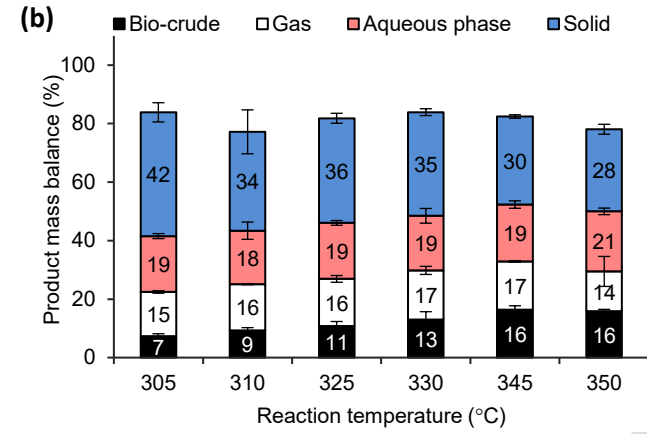
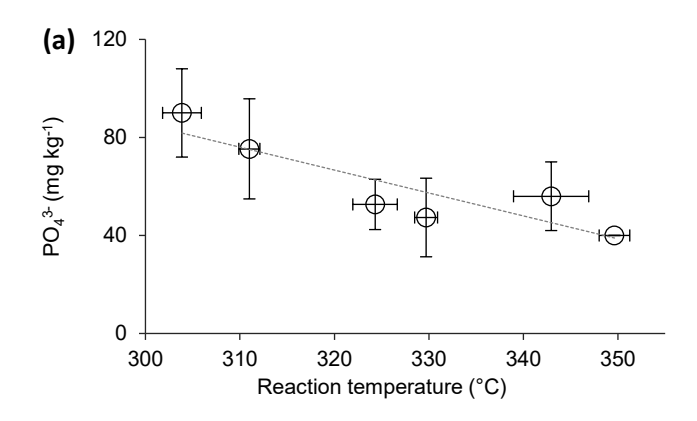


Figure 1 – Effect of a) the heating rate on the bio-crude yield from *A. nodosum* and b) reaction temperature on product distribution from the HTL of *A. nodosum* (mass fractions on dry basis). Non-closure of the mass balance is predominantly due to loss of some volatiles from the aqueous and bio-crude fractions on work up.



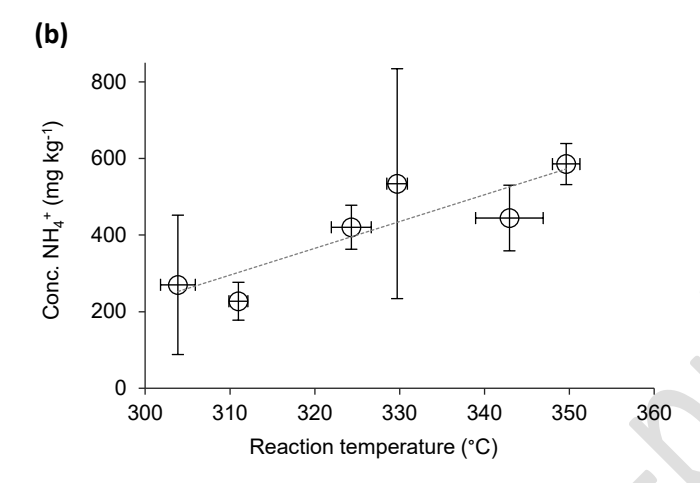


Figure 2 – Effect of reaction temperature on a) phosphate and b) ammonia concentration of aqueous phase from HTL of *A. nodosum*



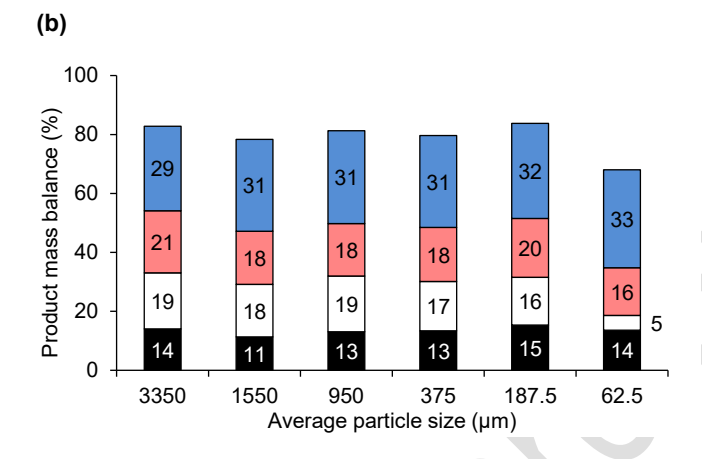


Figure 3 – a) *A. nodosum* ground particles with from left to right with an average particle size of 62.5, 187.5, 375, 950, 1550 μ m. **b)** Product mass balance from the HTL conversion of *A. nodosum* over variable particle size, at 345 °C (dry basis). The remaining fraction of the mass is assigned to volatile losses from the aqueous and bio-crude fractions on work up.

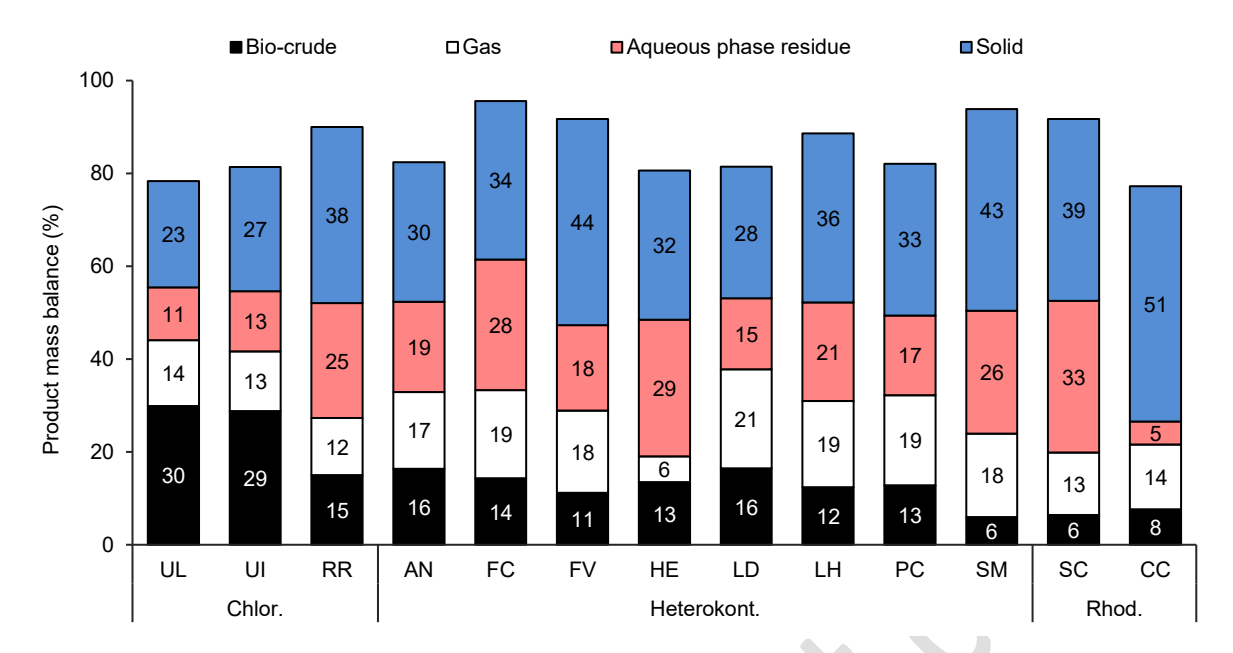


Figure 4 - Product distribution from HTL of 13 macroalgae species (345 °C; *ca.* 30 K min⁻¹). The remaining fraction of the mass is assigned to volatile losses from the aqueous and bio-crude fractions on work up.

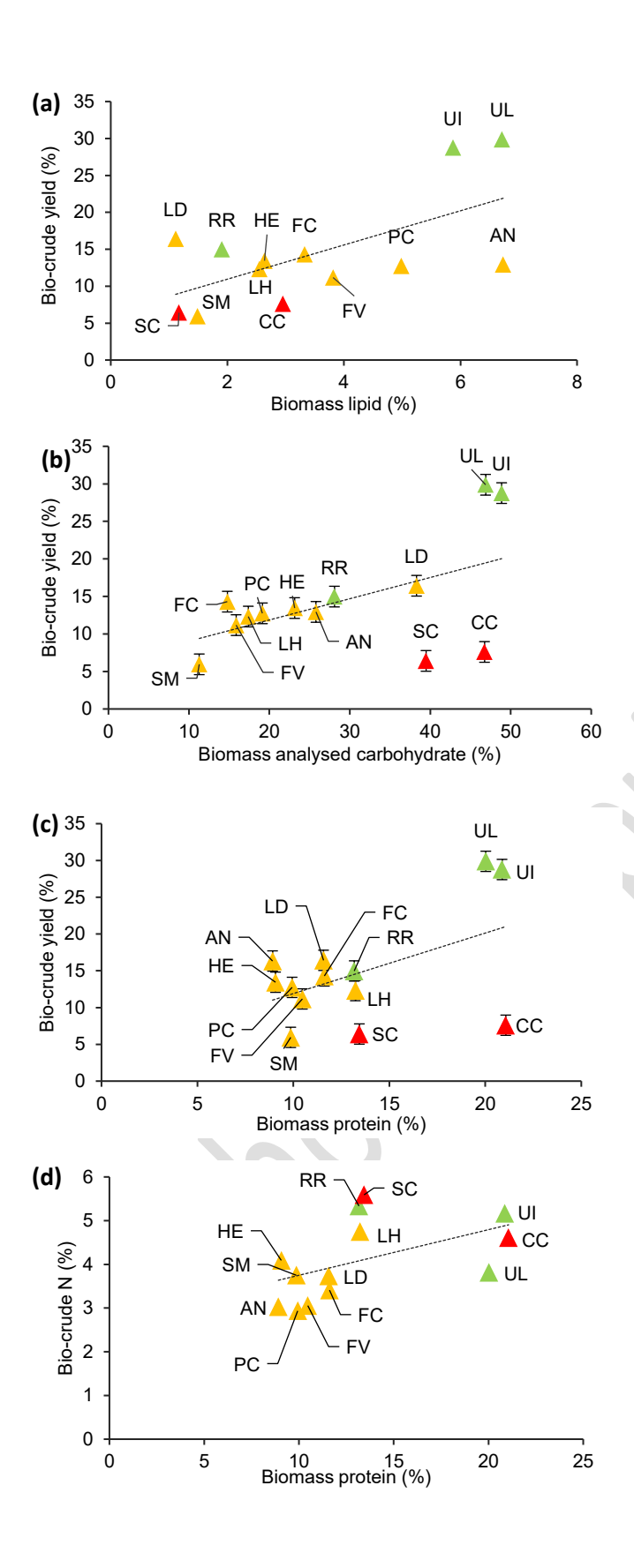


Figure 5 –Correlation between biomass biochemical composition and bio-crude yields and bio-crude nitrogen from HTL of 13 macroalgae species: a) biomass lipid vs. yield; b) biomass analysed carbohydrate vs. yield; c) biomass protein vs. yield; and d) biomass protein vs. bio-crude nitrogen

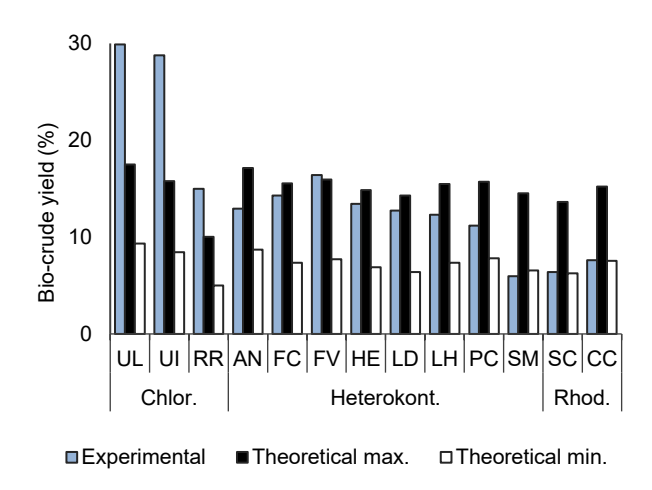
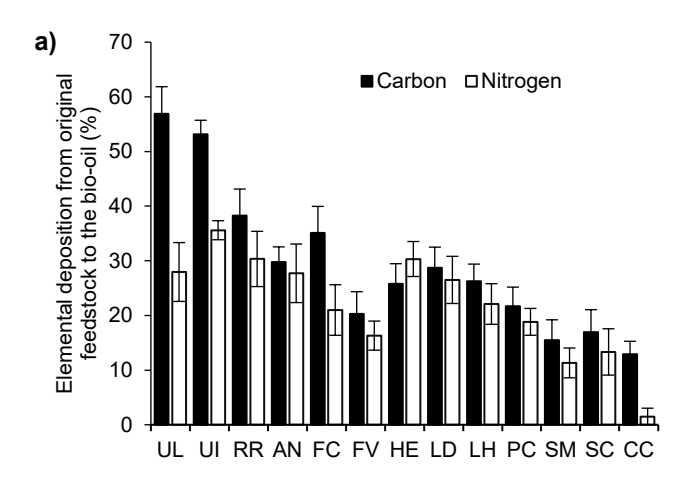


Figure 6 - Comparison of experimentally obtained bio-crude yields and yields calculated using the additive model proposed by Biller and Ross for HTL of 13 UK macroalgae species



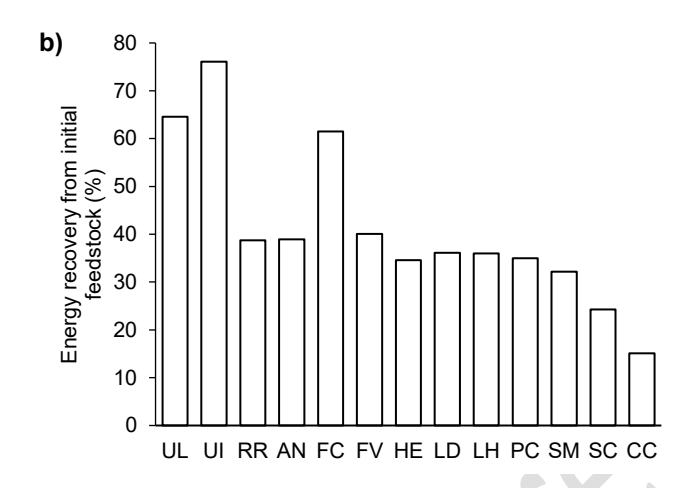
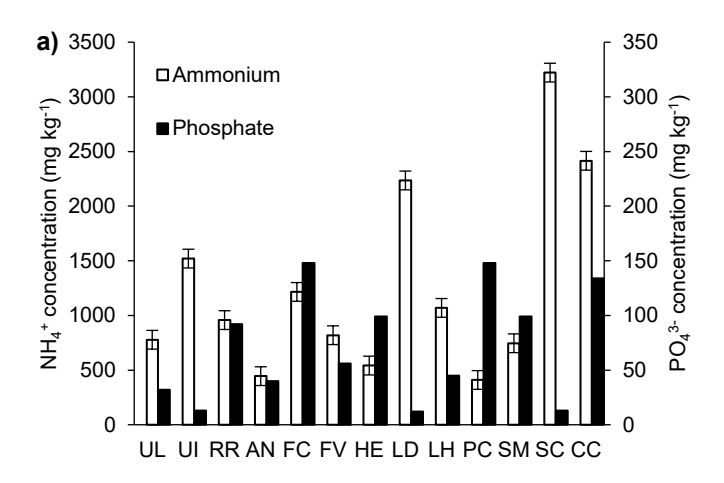


Figure 7 - a) Deposition of carbon and nitrogen from the initial feedstock into the bio-crude for the 13 species of macroalgae b) energy recovery of the bio-crude as a function of the biomass HHV.



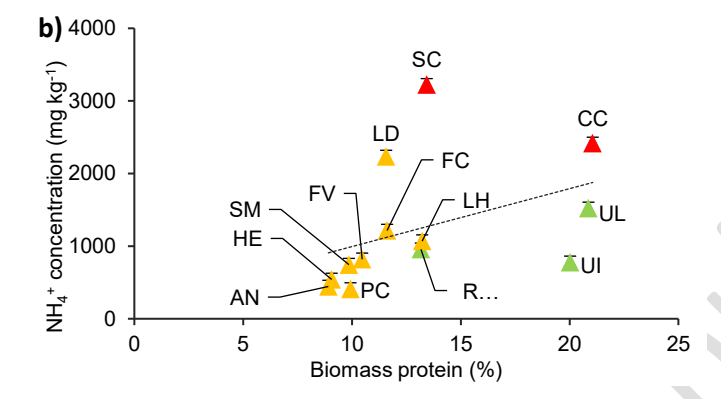


Figure 8 – a) Ammonia and phosphate deposition in the aqueous phase for each strain of macroalgae. b) Correlation between biomass protein and ammonia concentration in the aqueous phase from HTL of 13 macroalgae species

Table 1 – Biomass proximate, biochemical and ultimate analysis, and higher heating value (HHV)

Properties		Proximate (%)		Biochemical (%)				Ultimate (%)ª				(MJ kg ⁻¹)
	Type ^b	Moisture	Ashd	Proteine	Lipid ^f	Carb.g	Carb.h	С	Н	N	Oi	HHVg
UL	С	3.7	17.3	20.0	6.9	48.7	55.8	34.9	5.3	4.1	38.4	14.1
UI	С	7.7	24.5	20.9	5.9	48.9	48.8	35.2	5.8	4.2	30.4	15.4
RR	С	11.3	44.5	13.2	1.9	28.1	40.4	26.8	5.1	2.6	21.0	12.2
AN	Н	3.6	16.2	8.9	6.7	25.5	68.2	38.7	5.8	1.8	37.5	15.4
FC	Н	14.0	12.6	11.6	3.3	14.8	72.5	28.4	3.9	2.3	52.8	8.7
FV	Н	14.3	12.6	10.5	3.8	15.9	73.1	38.8	5.1	2.1	41.4	15.0
HE	Н	10.5	14.3	9.1	2.6	23.1	74.0	34.3	5.0	1.8	44.6	12.9
LD	Н	2.1	11.6	11.6	1.1	38.3	75.7	38.2	5.6	2.3	42.3	15.3
LH	Н	10.2	10.8	13.2	2.6	17.4	73.4	30.7	5.0	2.6	50.9	11.1
PC	Н	12.2	19.0	9.9	5.0	19.1	66.1	39.0	5.7	2.0	34.3	16.4
SM	Н	10.5	11.8	9.9	1.5	11.3	76.9	26.4	3.6	2.0	56.2	7.4
SC	R	6.0	17.1	13.4	1.2	39.5	68.3	25.3	3.5	2.7	51.4	7.3
CC	R	3.5	15.6	21.1	3.0	46.7	60.4	37.5	5.6	4.2	37.1	15.4

^a Average of two replicates; elemental mass fraction quoted on dry basis. ^b C – Chlorophyta (green); H – Heterokontophyta (brown), R – Rhodophyta (red).

^c Moisture mass fraction quoted on total biomass basis. ^d Ash mass fraction quoted on dry basis.. ^eProtein calculated from biomass N; mass fraction quoted on dry basis. ^f Analytical; mass fraction quoted on dry basis. ^g Calculated by difference; mass fraction quoted on dry basis. ^h Calculated by difference according to Jin et al. [36]; mass fraction quoted on dry basis. ⁱ Calculated from elemental composition using Channiwala and Parikh equation [44]